ACS OMEGA

http://pubs.acs.org/journal/acsodf

Article

Effect of Sintering Temperature on Properties of Carbon Fiber-Reinforced Titanium Matrix Composites

Changyu Hu, Jianhua Liu,* Lei Xu,* Lingfei Yu, and Beiping Zhu

Cite This: *ACS Omega* 2022, 7, 30087−30092

Read Online

ACCESS | Metrics & More | Article Recommendations | Supporting Information

ABSTRACT: Carbon fiber-reinforced titanium matrix composites were prepared by powder metallurgy. Carbon fiber (CF) powder and titanium (Ti) powder are mixed, pressed, and then sintered at a high temperature of 1300−1500 °C. The morphology and conductivity of carbon fiber-reinforced titanium matrix (Ti-CF) composites were studied. When the temperature range of the Ti-CF composites was from 1300 to 1500 °C, the porosity and resistivity first decreased and then increased. When the sintering temperature was 1350 °C, the diffraction peak of the sample was the strongest, the porosity was the smallest (4.16%), and the resistivity was the smallest (2.7 MΩ·mm). CFs have a very good strengthening effect on titanium-based composite materials.

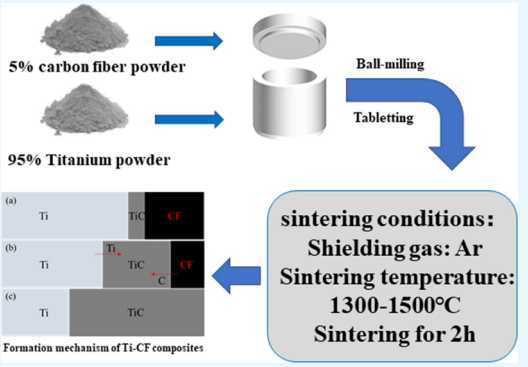

1. INTRODUCTION

Titanium and titanium composites, as lightweight structural materials with excellent performance, have high specific strength, specific rigidity, good processability, corrosion resistance, and high temperature resistance, and they have broad application prospects in many fields.[1−3] However, Young's modulus, wear resistance, and heat resistance of titanium materials are not as good as steel and nickel-based alloys.[4] Carbon fiber(CF) has a series of advantages such as high strength, high modulus, good lubricity, low thermal expansion coefficient, and excellent electrical and thermal conductivity, and they will not melt and soften at high temperatures and will not harden at low temperatures. The design concept of carbon fiber and other innovative materials reinforced metal matrix composites (MMCs) provides new ideas for the development of new materials with excellent mechanical properties. Some studies have achieved remarkable results using carbon fiber-reinforced Al,[5−9] Cu,[10−12] and Mg-[13−15] based MMCs.

There are not many reports on carbon fiber-reinforced titanium MMCs (Ti MMCs).[16] On the one hand, the performance of layered carbon fiber-reinforced titanium matrix composites was studied through the layering of CF cloth and titanium (Ti) powder. On the other hand, the reinforcement effect of chopped CF on titanium matrix composites was studied. In summary, CF cloth and chopped CFs only react with titanium on the surface, and the generated TiC is limited, and the reinforcing effect on the titanium matrix is limited. There are pores between the unreacted carbon fibers and the titanium matrix, resulting in an increase in porosity and a decrease in density.[17] Therefore, it is considered to use carbon fiber (CF) powder with a particle size similar to that of Ti powder as the carbon source to study the properties of carbon fiber-reinforced titanium matrix (Ti-CF) composites.

The in situ synthesis method is widely used in the preparation of MMCs because of its ability to form one or more fine reinforcing phases in the matrix, stable thermodynamic properties, and avoidance of adverse interfacial reactions. The methods for in-situ synthesis of titanium matrix composites generally include mechanical alloying, high-temperature self-propagating synthesis, powder metallurgical process, and so forth. In the mechanical alloying method, because the powder becomes finer during the ball milling process, its surface activity is improved, and it is in a state of extremely unstable thermodynamics and is prone to oxidation reactions. Although the high-temperature self-propagating synthesis method has a low reaction temperature and a small growth tendency of the reinforcing phase, which is beneficial to obtain an ultrafine reinforcing phase, the composites prepared using this method have porosity and low density. Andriyanov[18] used a high-temperature self-propagation method to prepare Ti-B-C ceramics, which have good structure and sufficiently high strength, but their total porosity is greater than 50%. The powder metallurgy technology has a sintering temperature lower than the melting point of the metal and a low degree of

Received: May 19, 2022
Accepted: August 11, 2022
Published: August 22, 2022

https://doi.org/10.1021/acsomega.2c03119
ACS Omega 2022, 7, 30087−30092

interface reaction. The advantage is being able to control the size and volume content of the reinforcing phase to avoid adverse reactions between the reinforcing phase and the matrix interface,[19] so powder metallurgy technology provides the possibility for the development of CF powder-reinforced Ti MMCs.

Nowadays, the choice of zinc-electrodeposited anode substrate material is a hot topic. The base material requires good mechanical strength, machinability, and good electrical conductivity. In this study, CF powder with a particle size similar to that of titanium powder was used as the carbon source. The Ti-CF composites were prepared using the powder metallurgy method, which can control the size and volume content of the reinforcing phase and avoid adverse reactions between the reinforcing phase and the matrix interface. The effects of different sintering temperatures on the morphology and electrical conductivity of Ti-CF composites were investigated. In addition, the distribution and reinforcement mechanism of the reinforcement phase in the titanium matrix were also investigated.

2. EXPERIMENTAL SECTION

2.1. Raw Materials. CF powder (99%, LISO COMPOSITE, Shanghai, China) is used as the raw material. Table 1

Table 1. Characteristics of CF Powder

powder	purity (%)	density (g/cm^3)	average particle size (μm)
CF	99.99	1.75	50

shows the characteristics of CF powder. The purity, density, and average particle size of CF powders are 99.99%, 1.75 g/cm^3, and 50 μm, respectively. Ti powder (99%, Aladdin, Shanghai, China) is used as the raw material. Table 2 shows the characteristics of Ti powder. The purity, density, and average particle size of Ti powders are 99.99%, 4.51 g/cm^3, and 48 μm, respectively.

Table 2. Characteristics of Ti Powder

powder	purity (%)	density (g/cm^3)	average particle size (μm)
Ti	99.99	4.51	48

The microscopic morphology and phase of the raw materials were observed by scanning electron microscopy (SEM, JSM6390, JEO) and X-ray diffraction (XRD, D/max-A, Rigaku). It can be seen from Figure 1a that the CF powder is a long strip with a length of about 50 μm. It can be seen from Figure 1b that the phase is CF. Figure 1c shows that Ti powder is in a typical irregular shape with a length of about 48 μm. It can be seen from Figure 1d that the phase is titanium.

2.2. Preparation of Ti-CF Composites. In order to achieve the best distribution of CF powder in the titanium-based powder, 5 wt % of CF powder was added to 2.8 g of Ti powder. The mixed powder was put into a mill (MSK-SFM-1-1L, Kejing) for 10 min, and 5 mL of absolute ethanol was added as a lubricant. The ball-milled samples were dried in a high-temperature drying oven and sieved. There are 72 balls in each can, and the charge is 2.95 g, among which the number of balls of 15, 11, 8, and 5 mm is 1, 5, 12, and 55 respectively. The pore diameter of the sieve is 60 mesh.

The mix powder was put into a cylindrical stainless-steel mold with a pressure of 40 MPa, and the pressure was

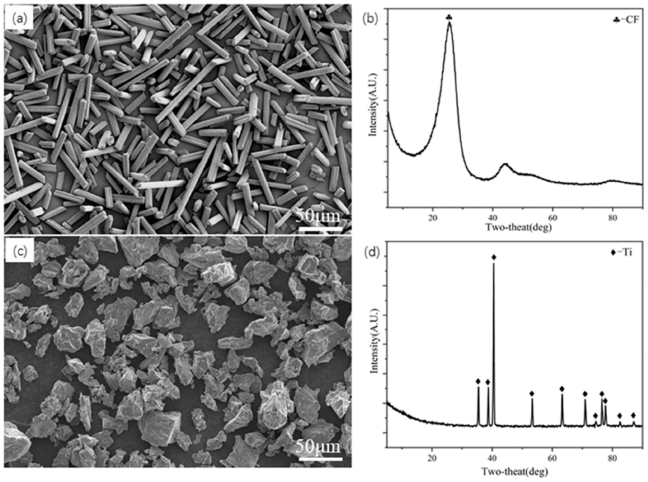

Figure 1. SEM and XRD of the starting material: (a) SEM of CF; (b) XRD of CF; (c) SEM of Ti; and (d) XRD of Ti.

maintained for 10 min. Sintering was carried out with a high-temperature tube furnace (GSL-1600x, Kejing) protected by an argon atmosphere, and the sintered samples were obtained with a diameter of 25 mm and a height of 2 mm. The sintering temperature was set to 1300, 1350, 1400, 1450, and 1500 °C, and the heating rate was 5 °C/min below 1000 °C and 3 °C/min above 1000 °C.

2.3. Characterization. The microscopic morphology of the samples was observed with a scanning electron microscope (JSM6390, JEO) with a voltage of 30 kV. In this experiment, an X-ray diffractometer (D/max-A, Rigaku) was used to analyze the phase of the sample by anodic CuKa (wavelength = 1.5418 Å) under 40 kV and 40 mA, and scanning was performed continuously at an angle of 10−90° for 10 min. The conductivity of the sample was measured with a resistivity tester (FT-340, ROOKO). The square four-probe and square resistance mode are selected, and the distance between the probes is 2.35 mm. The sample thickness is measured with a Vernier caliper, and its value is input.

The beaker filled with deionized water is placed on a resistance furnace and heated to boiling, and the sample is immersed in deionized water and suspended for 5 min to eliminate the gas in the sample. The porosity is calculated by formula 1.

$$K = (m_2 - m_1)/m_1 \quad (1)$$

In the formula, m_1 is the dry weight of the sample in air; m_2 is the mass of the sample after boiling for 5 min.[20]

3. RESULTS AND DISCUSSION

3.1. Thermodynamic Analysis of the Ti-C System. For the Ti-C system, Ti-CF composites have been prepared through the reaction formula 2. Researchers such as Lv and co-workers[21,22] used thermodynamic parameters (formulas 3 and 4) to calculate the enthalpy of reaction formation ΔH and Gibbs free energy ΔG.

$$\mathrm{Ti} + \mathrm{C} = \mathrm{TiC} \quad (2)$$

When the system temperature was lower than 1939 K (1666 °C),

$$\Delta H = -184571.8 + 5.042\,T - 2.425 \times 10^{-3}\,T^2 - 1.958 \times 10^{6}/T \quad (3)$$

https://doi.org/10.1021/acsomega.2c03119
ACS Omega 2022, 7, 30087−30092

$$\Delta G = -184571.8 - 5.042\ T\ln T + 41.382\ T + 2.425 \times 10^{-3}\ T^2 - 9.79 \times 10^5/T \quad (4)$$

By calculating the values of ΔG and ΔH at different temperatures, the change curve of ΔG and ΔH with temperature is shown in Figure 2. In the research temperature

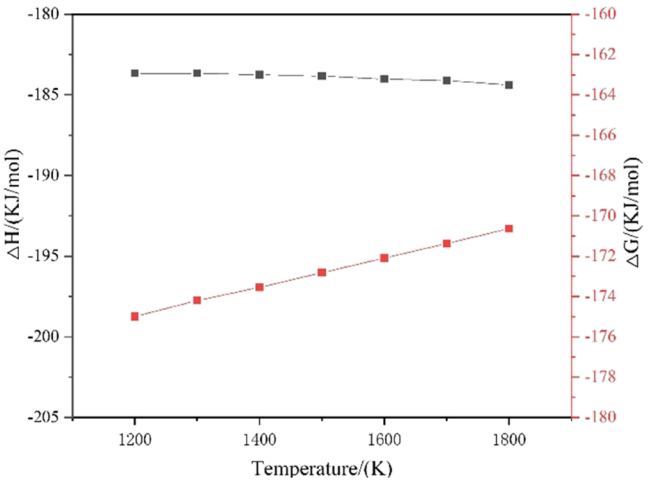

Figure 2. ΔG, ΔH curve with temperature.

range (1300, 1350, 1400, 1450, and 1500 °C), ΔG is negative, indicating that the reaction 2 is thermodynamically feasible and can proceed spontaneously; The ΔH value is negative, indicating that the reaction is exothermic, and a lot of heat will be released during the reaction.

3.2. Phase Analysis. It can be seen from Figure 3 that the XRD peak of TiC appears newly, but the X-ray diffraction peak

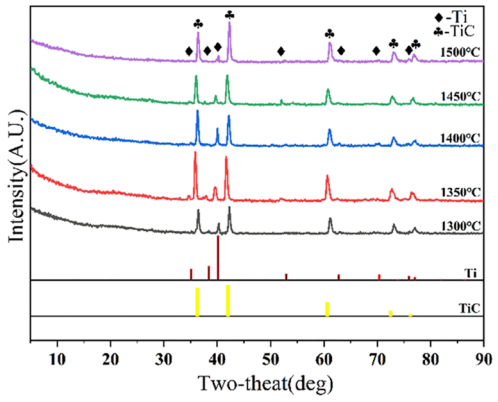

Figure 3. XRD of Ti-CF composites at different temperatures.

of CF is absent. From this, it can be inferred that the CF reacts with titanium to form TiC (The XRD database used is pdf2-2016). Because the smaller the phase particle size, the wider is the diffraction peak.[23−25] As the temperature increases, the width of the diffraction peak first increases and then decreases, which indicates that the size of the self-generated TiC grains in the Ti-CF composites first decreases and then increases. When the sintering temperature is 1300 °C, the diffraction peak intensity of TiC is the lowest, and when the sintering temperature is 1350 °C, the diffraction peak of TiC is the highest and sharpest. When the sintering temperature is greater than 1350 °C, the intensity of the diffraction peak becomes lower. It shows that 1350 °C is the critical temperature point, which is beneficial to the formation of TiC and makes the effect of TiC crystal grain generation have a significant change.

3.3. Microstructural Analysis. Figure 4 shows the SEM of samples at different temperatures. It shows that the size of

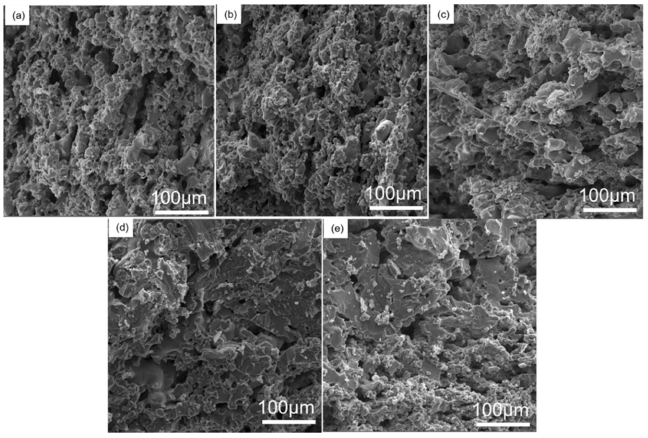

Figure 4. SEM of samples at different temperatures. (a)1300 °C; (b) 1350 °C; (c) 1400 °C; (d) 1450 °C; and (e) 1500 °C.

pores decreases first and then increases from 1300 to 1500 °C at 1300−1350 °C; large pores in the sample are divided into small pores. Above 1350 °C, the number of pores decreases, but the volume of pores increases. At 1350 °C, the volume of pores is the smallest. Figure 5 is the surface scan of the sample

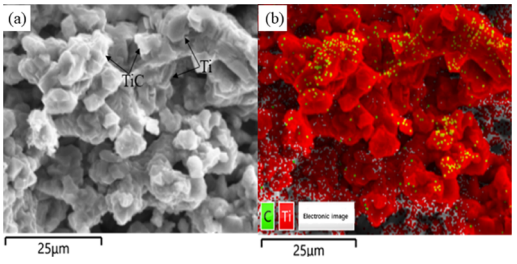

Figure 5. Surface scan of the sample obtained at 1500 °C: (a) SEM of Ti-CF composites at 1500 °C; (b) scanning image of Ti-CF composites at 1500 °C.

obtained at 1500 °C. It can be seen from Figure 5 that C is unevenly distributed on the titanium. Figure 6 is the point scan of the sample obtained at 1400 °C. There are only titanium elements in point 1, and there are titanium and carbon elements in point 2. Figures 4−6 show that the TiC layer formed on the Ti surface appears in the form of small particles with an irregular crystal morphology.

3.4. Porosity Analysis. Figure 7 shows the porosity of Ti-CF composite materials obtained at different temperatures. It shows that the porosity first decreases and then increases. From 1300 to 1350 °C, At this time, the pressure of the internal voids of the sample is greater than the external pressure, gas flows out of the voids, and the porosity decreases. However, from 1350 to 1500 °C, because of the different thermal expansion coefficients of Ti and TiC, the mass percentage of CF is only 5%. Combined with Figure 5b, it can be seen that the distribution of CF is uneven, so that the thermal expansion of each part of the sample is uneven. Certain voids are formed on the surface of the sample, so the porosity increases. Therefore, too high sintering temperature

https://doi.org/10.1021/acsomega.2c03119
ACS Omega 2022, 7, 30087−30092

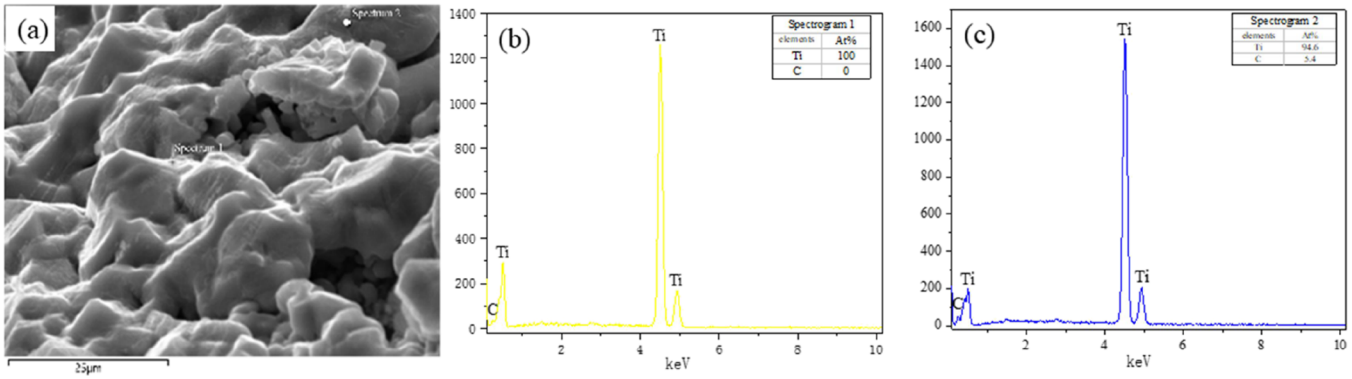

Figure 6. Point scan of the sample obtained at 1400 °C: (a) Spot sweep energy spectrum of Ti-CF composites at 1400 °C; (b) atomic percentage diagram of point 1; (c) atomic percentage diagram of point 2.

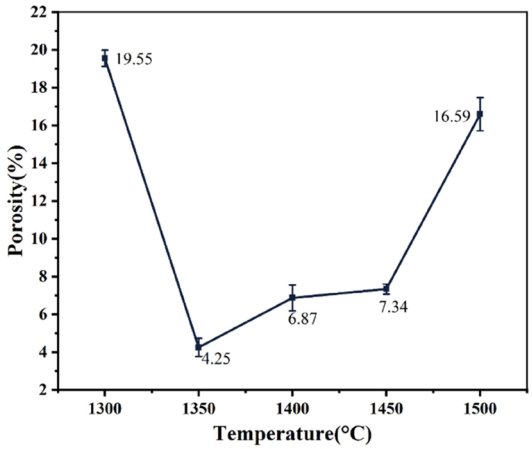

Figure 7. Porosity of Ti-CF composites at different temperatures.

will cause deterioration of the mechanical properties of Ti-CF composites. Therefore, the porosity of the sample obtained at 1350 °C is the smallest and is only 4.16%, which is 15.45% lower than that of the sample obtained at 1300 °C.

3.5. Resistivity Analysis. Figure 8 shows the resistivity of Ti-CF composite materials obtained at different temperatures. It shows that the resistivity first decreases and then increases as the temperature increases. Combined with the analysis in Figures 4 and 7, from 1300 to 1350 °C, the TiC and Ti grains become fine and compact. Also, the porosity decreases and the density increases so that the resistivity of the Ti-CF composite material decreases. However, from 1350 to 1500 °C, first, the porosity increases and the sample has some large voids, failing to form a good conductive path. Second, the conductivity of TiC decreases as the temperature increases.[26] Therefore, the resistivity increases. Compared with 1300 and 1500 °C, the resistivity of the Ti-CF composite material obtained at 1350 °C is reduced by nearly 2.5 times and 3 times. Therefore, the sample has the smallest resistivity at 1350 °C, and the resistivity is only 2.7 MΩ·mm.

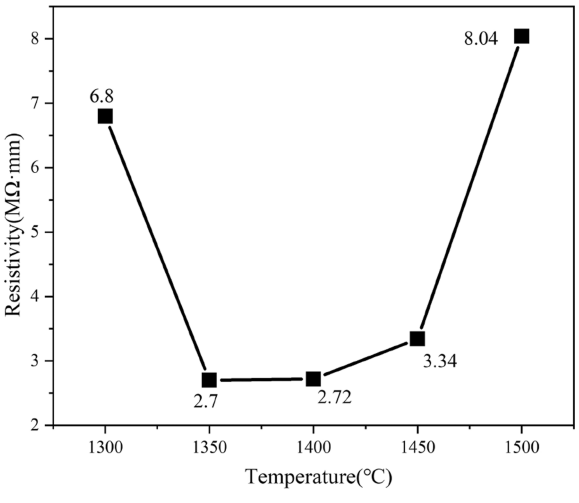

Figure 8. Resistivity of Ti-CF composites at different temperatures.

3.6. Reaction Mechanism. According to the above introduction, at the sintering temperature of this experiment, the reaction of Ti + C = TiC meets the thermodynamic conditions and can cause an exothermic reaction. The formation reaction of titanium carbide is a solid−solid reaction. The schematic diagram of the synthesis mechanism of Ti-CF composites is shown in Figure 9. The experimental reaction can be summarized in three stages: Figure 9a shows that Ti atoms in the matrix and C atoms in the surface layer form a TiC layer. Figure 9b shows that the structure of the CF surface has been destroyed, and the activity of some C atoms increases. Figure 9c shows that the overall structure of the CF is largely destroyed, Ti atoms and C atoms are mutually diffused with TiC as a bridge, and finally, all the C atoms in the CF participate in the reaction to form TiC.

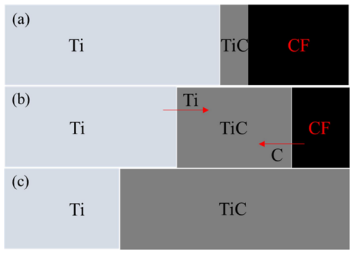

Figure 9. Schematic diagram of the synthesis mechanism of Ti-CF composites: (a) first stage of reaction; (b) second stage of reaction; and (c) third stage of reaction.

4. CONCLUSIONS

Carbon fiber powder with an average particle size 50 μm is used as the raw material, and Ti-CF composites are prepared by powder metallurgy.

https://doi.org/10.1021/acsomega.2c03119
ACS Omega 2022, 7, 30087−30092

(1) When the temperature is 1300−1500 °C, ΔG of titanium carbide produced by Ti and CF powder is less than 0, which is thermodynamically feasible.
(2) The optimal sintering temperature of the Ti-CF composite material is 1350 °C. The Ti-CF composite material obtained at the optimal sintering temperature has the smallest porosity (4.16%) and the smallest resistivity (2.7 MΩ·mm).

■ ASSOCIATED CONTENT

Supporting Information

The Supporting Information is available free of charge at https://pubs.acs.org/doi/10.1021/acsomega.2c03119.

Characteristics of CF powder and Ti powder; ΔG, ΔH of the Ti-C system at different temperatures; XRD, SEM, porosity, and resistivity of Ti-CF composites at different temperatures; and schematic diagram of the synthesis mechanism of Ti-CF composites at different temperatures (PDF)

■ AUTHOR INFORMATION

Corresponding Authors

Jianhua Liu − *Faculty of Metallurgical and Energy Engineering and State Key Laboratory of Complex Nonferrous Metal Resources Clean Utilization, Kunming University of Science and Technology, Kunming 650093, China*; orcid.org/0000-0003-0556-8941; Email: liujianhua501050@163.com

Lei Xu − *Faculty of Metallurgical and Energy Engineering, Kunming University of Science and Technology, Kunming 650093, China*; Email: xu_lei@kust.edu.cn

Authors

Changyu Hu − *Faculty of Metallurgical and Energy Engineering, Kunming University of Science and Technology, Kunming 650093, China*

Lingfei Yu − *Zinc & Indium smelting co, Ltd Wenshan Yunxi, Wenshan 663700, China*

Beiping Zhu − *Zinc & Indium smelting co, Ltd Wenshan Yunxi, Wenshan 663700, China*

Complete contact information is available at: https://pubs.acs.org/10.1021/acsomega.2c03119

Notes

The authors declare no competing financial interest.

■ ACKNOWLEDGMENTS

This work was supported by Yunnan Fundamental Research Projects (grant No. 202001AT070203) and the construction of high-level talents of the Kunming University of Science and Technology (No. 1411909413).

■ REFERENCES

(1) Mani, S.; Palanisamy, C.; Murugesan, M.; Balasubramanian, R. Estimation of distinctive mechanical properties of spark plasma sintered titanium-titanium boride composites through nano-indentation technique. *Int. J. Mater. Res.* **2015**, *106*, 1182−1188.
(2) Abkowitz, S.; Abkowitz, S. M.; Fisher, H.; Schwartz, P. J. CermeTi (R) discontinuously reinforced Ti-matrix composites: Manufacturing, properties, and applications. *Jom.* **2004**, *56*, 37−41.
(3) Qu, X. H.; Xiao, P. A.; Zhu, B. J.; Qin, M. L. Progress in research and development of high-temperature titanium alloys and particulate-reinforced titanium matrix composites. *Rare Metal Mat. Eng.* **2001**, *30*, 161−165.
(4) Kuzumaki, T.; Ujiie, O.; Ichinose, H.; Ito, K. Mechanical characteristics and preparation of carbon nanotube fiber-reinforced Ti composite. *Adv. Eng. Mater.* **2000**, *2*, 416−418.
(5) Singh, B. B.; Balasubramanian, M. Processing and properties of copper-coated carbon fiber reinforced aluminium alloy composites. *Mat. Sci. Eng. A Struct.* **2009**, *209*, 2104−2110.
(6) Kim, J. G.; Kim, H. C.; Kwon, J. B.; Shin, D. K.; Lee, J. J.; Huh, H. Tensile behavior of aluminum/carbon fiber reinforced polymer hybrid composites at intermediate strain rates. *J. Compos. Mater.* **2015**, *49*, 1179−1193.
(7) Khayamdar, M.; Khoramishad, H. The effect of metallic fiber geometry and multi-walled carbon nanotubes on the mechanical behavior of aluminum fiber-reinforced composite adhesive joints. *Proc. Inst. Mech. Eng. L: J. Mat.* **2021**, *235*, 949−957.
(8) Galyshev, S.; Galyshev, S.; Gallyamova, R.; Khodos, I.; Musin, F. On the liquid-phase technology of carbon fiber/aluminum matrix composites. *Int. J. Min. Met. Mater.* **2019**, *26*, 1578−1584.
(9) Lalet, G.; Kurita, H.; Miyazaki, T.; Kawasaki, A.; Silvain, J. F. Microstructure of a carbon fiber-reinforced aluminum matrix composite fabricated by spark plasma sintering in various pulse conditions. *J. Mater. Sci.* **2014**, *49*, 3268−3275.
(10) Wan, Y. Z.; Wang, Y. L.; Luo, H. L.; Cheng, G. X. Relationship between elastic behavior and interfacial bonding strength for carbon fiber reinforced copper composites. *J. Mater. Sci. Lett.* **2000**, *19*, 183−184.
(11) Yang, L. W.; Dong, Y.; Wang, R. J. Wear and mechanical properties of short carbon fiber reinforced copper matrix composites. In *Key Engineering Materials*; Trans Tech Publications, Ltd.: 2011; Vol. *474*, pp. 1605−1606.
(12) Chen, S. Y.; Li, X. R.; Bi, Y. N.; Wellburn, D.; Liang, J.; Liu, C. S. Preparation of the carbon fiber/Cu alloy matrix self-lubricating composite materials. In *Applied Mechanics and Materials*; Trans Tech Publications, Ltd.: 2014; Vol. *670*, pp. 164−167.
(13) Hufenbach, W.; Andrich, M.; Langkamp, A.; Czulak, A. Fabrication technology and material characterization of carbon fiber reinforced magnesium. *J. Mater. Process Technol.* **2006**, *175*, 218−224.
(14) Cortes, P.; Cantwell, W. J. Fracture properties of a fiber-metal laminates based on magnesium alloy. *J. Mater. Sci.* **2004**, *39*, 1081−1083.
(15) Korner, C.; Schaff, W.; Ottmuller, M.; Singer, R. F. Carbon long fiber reinforced magnesium alloys. *Adv. Eng. Mater.* **2000**, *2*, 327−337.
(16) Li, S. F.; Sun, B.; IMAI, H.; Mimoto, T.; Kondoh, K. Powder metallurgy titanium metal matrix composites reinforced with carbon nanotubes and graphite. *Compos. A Appl. Sci. Manuf.* **2013**, *48*, 57−66.
(17) Kiehn, J.; Bohm, E.; Kainer, K. U. Deformation of continuous carbon fiber reinforced Mg-alloys by thermally induced stresses. In *Key Engineering Materials*; Trans Tech Publications, Ltd.: 1997; Vol. *127*, pp. 861−868.
(18) Andriyanov, D. I.; Amosov, A. P.; Samboruk, A. R.; Davydov, D. M.; Ishchenko, V. S. Development of porous composite self-propagating high-temperature ceramics of the Ti-B-C system. *Russ. J. Non-Ferrous Metals* **2014**, *55*, 485−488.
(19) Yang, Z.; Lu, W.; Zhao, L.; Qin, J.; Zhang, D. Microstructure and mechanical property of in-situ synthesized multiple-reinforced (TiB+TiC+La_2O_3)/Ti composites. *J. Alloy Compd.* **2008**, *455*, 210−214.
(20) Lin, L.; Zhang, X.; Chen, J.; Mu, Y. F.; Li, X. M. A novel random void model and its application in predicting void content of composites based on ultrasonic attenuation coefficient. *Appl. Phys. A Mater.* **2011**, *103*, 1153−1157.
(21) Lv, W. J.; Zhang, X. N.; Zhang, D.; Wu, R. J.; Bain, Y. Q.; Fang, P. W. Growth mechanism of in-situ synthesized TiC/Ti-based composite reinforcement. *Acta Metall. Sin.* **1999**, *5*, 536−540.
(22) Sun, S. Y.; Lv, W. J. Effects of Trace Reinforcements on Microstructure of TC18 Titanium Matrix Composite. *Rare Metal Mat. Eng.* **2017**, *46*, 606−611.

(23) Lee, S. H. In-situ Synthesis and Investment Casting of Titanium Matrix (TiC+TiB) Hybrid Composites. *J. Korea Foundry Soc.* **2004**, *24*, 159−164.
(24) Wang, T. R.; Ma, F. C.; Li, P.; Li, W.; Liu, X. K.; Lv, W. J.; Zhang, D. High temperature mechanical properties and strengthening mechanism of in-situ (TiB+TiC)/Ti-1100 composite. *J. Mater. Sci. Eng.* **2018**, *36*, 432−437.
(25) Yang, Y. C.; Yu, P.; Lu, X.; Yu, A. H.; Hui, T. L.; Liu, Y. J. Research progress of particle-reinforced titanium matrix composites prepared by powder metallurgy. *Powder Metal. Technol.* **2020**, *38*, 150−158.
(26) Li, S. F.; Kondoh, K.; Imai, H.; Chen, B.; Jia, L.; Umeda, J.; Fu, Y. B. Strengthening behavior of in situ-synthesized (TiC-TiB)/Ti composites by powder metallurgy and hot extrusion. *Mater Des.* **2016**, *95*, 127−132.

https://doi.org/10.1021/acsomega.2c03119
ACS Omega 2022, 7, 30087−30092